Advanced Wind Tunnel Boundary Simulation for Kevlar Wall Aeroacoustic Wind Tunnels

Devenport, William; Brown, Ken; Borgoltz , Aurelien ; Paterson, Eric; Bak, Christian; Sørensen, Niels N.; Olsen, Anders Smærup; Gaunaa, Mac; Fischer, Andreas; Grinderslev, Christian

Publication date:
2018

Document Version
Publisher's PDF, also known as Version of record

Advanced Wind Tunnel Boundary Simulation for Kevlar Wall Aeroacoustic Wind Tunnels

William Devenport, Ken Brown, Aurelien Borgoltz and Eric Paterson
Center for Renewable Energy and Aerodynamic Technology
Department of Aerospace and Ocean Engineering, Virginia Tech, Blacksburg VA24060 USA
devenport@vt.edu

Christian Bak, Niels Sørensen, Anders Olsen, Mac Gaunaa,
Andreas Fischer, Christian Grinderslev
Technical University of Denmark, 4000 Roskilde, Denmark
chba@dtu.dk

ABSTRACT

This paper presents tests carried out in the Virginia Tech Stability Wind Tunnel with Kevlar walls to allow for aeroacoustic measurements. Two-dimensional Computational Fluid Dynamics (CFD) calculations using the EllipSys2D solver were carried out to investigate the impact of no-slip condition, porosity, and flexibility of the simulated walls on the aerodynamics of a 0.9m-chord DU91-W250 airfoil at a Reynolds number of 3M. The accuracy of the airfoil simulation was first benchmarked against the experimental data, including data obtained in the Stability Tunnel hard-wall test section, and then the impact of boundary conditions on the simulation of the Kevlar test-section was investigated. The CFD was able to reproduce most of the airfoil characteristics (its lift, pressure distributions, and velocity profiles measured through the airfoil wake) as well as the growth of the wind tunnel wall boundary layers downstream of the model. All three boundary condition parameters (porosity, deflection, and no-slip condition) were found to have a high impact on the accuracy of the simulation. In particular, the no-slip condition was found to influence the pressure difference across the Kevlar walls and thus the transpiration through them, making it important in the aerodynamic correction process. The comparisons also highlighted some issues that need to be investigated further. The CFD consistently under-predicted drag while predicting transition locations upstream of those measured. Calculations also showed slightly larger blockage effects on the airfoil pressure distributions than those measured. This may be the result of an over-estimate of the blockage associated with transpiration through the wall.

1.0 INTRODUCTION

Kevlar-walled test sections represent an important emerging technology in the area of aeroacoustic testing. In this arrangement, large Kevlar screens are used in place of wind tunnel walls. The Kevlar is transparent to sound over a broad frequency range and almost impervious to flow. The primary effect is to combine the desirable acoustic characteristics of an open jet wind tunnel, with the comparatively low levels of aerodynamic interference associated with a hard wall test section. Secondary effects include stabilizing of the jet allowing for a much longer test section and much closer placement of acoustic sensors to the test article, the combined effect of which is a considerable gain in acoustic signal to noise ratio. The Kevlar concept was introduced some 12 years ago at the Virginia Tech Stability Wind Tunnel [1]. It has since been adopted by a number of other facilities including the 2-m tunnel at JAXA [2] (Japan), the 2.44-m Anechoic Flow Facility at David Taylor Research Center in Maryland (US) and, most recently, the new 2 by 3-m aeroacoustic wind tunnel currently

under construction at Technical University of Denmark (DTU), the Poul la Cour Tunnel. This technology is also undergoing testing for application to facilities at NASA Langley.

During operation a model placed in the test section experiences the effects of confinement as a result of both the aerodynamic and structural behavior of the Kevlar side walls. Devenport *et al.* [1] identified three distinct effects, Fig. 1. Firstly, the flow around a model placed in the test section produces pressure differences across the Kevlar walls. Since the walls are porous (typical open area ratio is a few percent), these generate transpiration through the walls. The relationship between the transpiration velocity and the pressure difference appears independent of tangential flow on one side of the Kevlar and can be determined for all conditions by calibration in an independent facility. The transpiration velocity deflects the free stream from its nominal axial direction producing an effective angle of attack change. Secondly, the pressure difference across the Kevlar walls causes them to elastically deflect into the test section in regions where the model is producing low pressures, and outward where pressures are increased. These deflections are counter to the local streamline curvature and thus reduce the effective test section height. This increases solid and wake blockage effects, particularly at high lift. Thirdly, the porosity of the walls allows for a small amount of flow to be diverted around the model by passing outside of the test section through the porous walls. This acts to decrease blockage effects at low lift conditions.

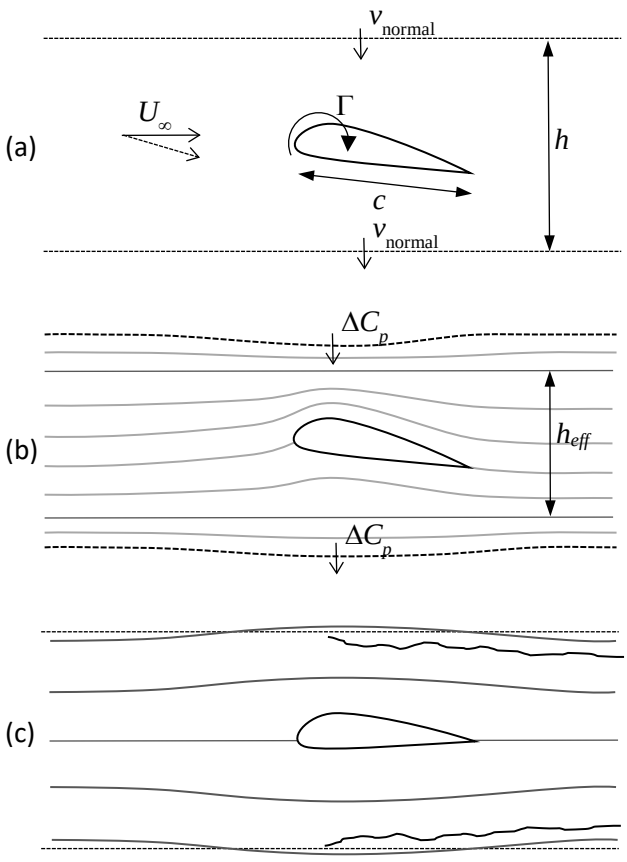

Figure 1. Schematics showing the origins of aerodynamic corrections in porous flexible wall tunnels. (a) The porosity correction to angle of attack. (b) Increase in the blockage correction (confinement) due to deflection of the acoustic windows. (c) Reduction in the blockage correction due to diversion of the flow out of the test section. From [1].

Aerodynamic corrections for this type of facility have to date involved ideal flow solutions in which a vortex panel method is used to model the influence of the flexible porous walls, with a normal velocity boundary condition at the walls determined by the computed pressure there and the empirically determined relation between the Kevlar transpiration velocity and pressure difference [1]. The panel method is coupled with a uniform-tension membrane model that adjusts the position of the walls in accordance with the pressures and the nominal mechanical properties of the Kevlar fabric.

This method has been demonstrated, at least for two-dimensional airfoil testing, to provide accurate *a priori* aerodynamic corrections over a range of conditions. However, this method clearly does not represent many complexities in the test section operation, complexities that may come to dominate aerodynamic corrections or performance with different model types or at more extreme conditions.

Recent work by Brown [3] examined in detail the assumptions behind this correction method, focusing predominantly on the behavior of the Kevlar itself. He found the effective mechanical properties of the Kevlar to be quite different than their nominal values due to characteristics of the fabric weave, as opposed to those of

the Kevlar filaments themselves. He also found a possible fourth source of aerodynamic correction – a change in angle of attack introduced when deformation is not symmetric with respect to the lift axis of the model.

In this paper we have used Computational Fluid Dynamics (CFD) to focus on the flow behavior of a Kevlar walled wind tunnel test section. This paper is part of a long term collaboration to establish validated detailed digital models of the Stability Wind Tunnel at Virginia Tech and the Poul la Cour Wind Tunnel at DTU. In this paper our specific fluid dynamic interest is in understanding how the boundary layers on the Kevlar walls can be modelled and what impact they have on model testing in the wind tunnel, directly by affecting blockage and flow deflection, and indirectly by altering wall shape. This study has necessarily forced us also to face broader issues concerning the use of advanced simulation in wind tunnel testing. Specifically (1) the origin and relative importance of the physical effects controlling the aerodynamic corrections, and (2) the complications involved in matching CFD boundary conditions and solutions to actual test conditions. Our long term interest is also in revealing possible avenues for using CFD directly in estimating more accurate far-field corrections to free flight conditions.

The experimental test case that forms the focus of the studies performed in this paper is the flow over a full span DU91-W250 airfoil. This model has been tested in both the Kevlar-wall and hard wall test sections of the Stability Tunnel. Experimental configurations are described in section 2. Two-dimensional CFD calculations have been performed for the flow past this airfoil in free flight and in the wind tunnel with a variety of wall boundary conditions using both the EllipSys code [4-6] developed at DTU. The method is described in section 3 and results are discussed in comparison to experimental data in section 4.

2.0 EXPERIMENTAL FACILITY AND TEST CASE

The Stability Tunnel is a low-speed closed circuit wind tunnel used for a mix of commercial testing, research and educational experiments on the campus of Virginia Tech in Blacksburg Virginia. The facility, driven by a 600hp fan, can generate speeds of up to 80 m/s through its 7.3-m long, 1.85-m square test sections. Flow through

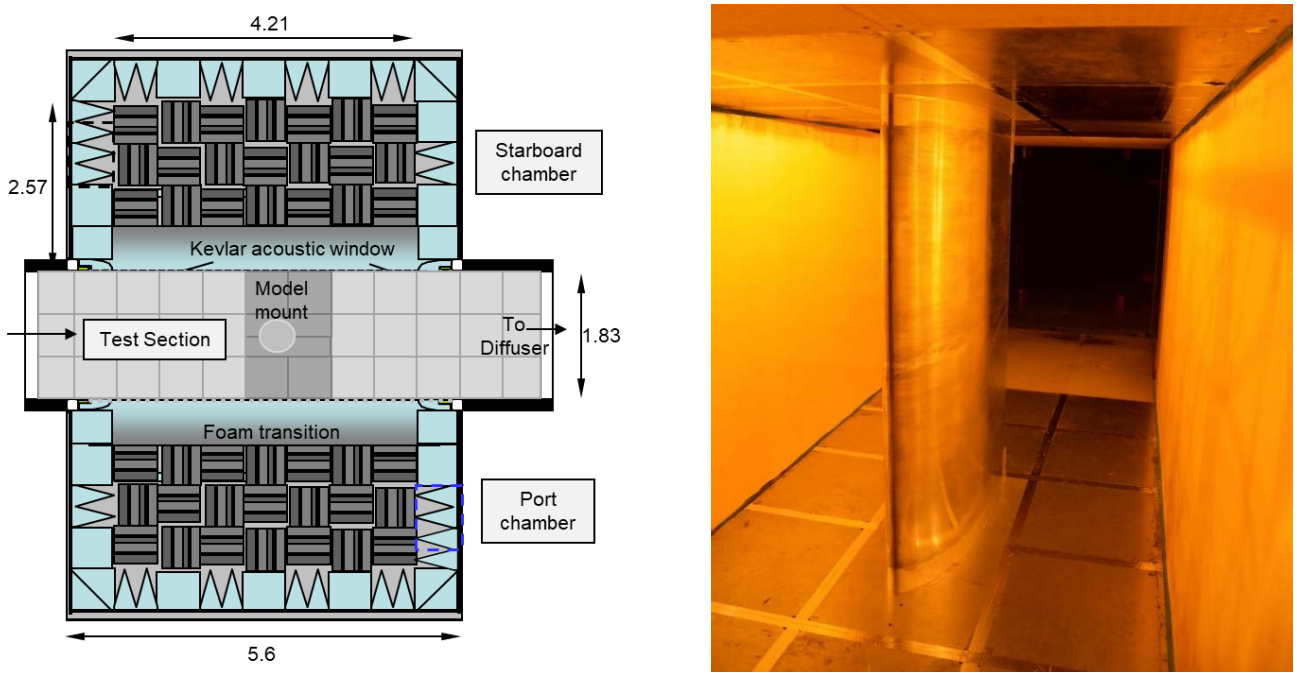

Figure 2 (a) Cross section through the Kevlar-wall test section and anechoic chambers as seen from above, dimensions in meters, from [1]. (b) View of the DU91-W250 model in the test section as seen from upstream adjacent to the port-side acoustic window.

the empty test sections is closely uniform and of very low turbulence intensity, increasing from 0.021% at 21 m/s to 0.031% at 57 m/s.

Two test sections are available. The hard wall "aerodynamic" test section has walls formed from a sequence of aluminum panels. Two dimensional models are mounted spanwise vertical at the center of the test section and rotated to angle of attack about an axis 3.56 m downstream of the test section entrance. Angle of attack can be varied under computer control and is sensed directly using four Acuity AR700-32 laser distance sensors embedded in the test section walls. A total of 140 pressure taps are mounted in the side walls of the test section are used for non-contact lift measurements as well as monitoring of the wall boundary condition.

The Kevlar-wall "aeroacoustic" test section (Fig. 2) replicates the same interior dimensions as the hard wall test section. The side walls of this test section, however, include 4.2-m long openings that span the full 1.85-m test section height. These openings are covered using tensioned Kevlar cloth that is almost transparent to sound and only slightly porous to the flow. Sound generated by models in the test section travels out through these acoustic windows into anechoic chambers that flank the test section. Most acoustic measurements are made using microphones placed in these chambers. Kevlar 120 cloth is used for the windows. This is a scrim made from a plain weave of Kevlar 49 fiber with 13.4 threads per centimeter in both warp and weft directions. For the tests reported here, cloth provided by EAS Fiberglas Company was used with an open area ration of 1.8%, weight of 58 g per square meter, thickness of 0.08 mm, and equivalent membrane thickness of 0.021 mm [3]. Nominal bulk modulus of Kevlar 49 is 126 GPa but the effective modulus of the Kevlar 120 scrim is 13.3 and 31.2 GPa in the warp and weft directions, respectively [3]. The Kevlar forming the acoustic windows is supported on tensioning frames under a nominal no-flow tension of 1500 N/m. The ceiling and floor of the acoustic test section are formed, primarily, from perforated metal panels backed by 0.46-m acoustic wedges to serve as sound absorbers. The perforated panels are covered with additional Kevlar cloth in order to form a low-noise flow surface. Two-dimensional airfoil models are mounted in the same position as in the hard wall test section and identical angle of attack control and sensing systems are used. Floor and ceiling panels in the immediate vicinity of the model are replaced with impermeable aluminum panels (Fig. 2(b)) so as to avoid flow through the acoustic treatment driven by model-generated pressure gradients.

Transpiration through the Kevlar scrim is characterized via pressure drop measurements made in purpose built calibration rig [3]. The resulting empirical relationship for the average flow velocity through the Kevlar v in terms of the pressure difference Δp across it is, in dimensional form,

$$v = k_c \Delta p^{0.5} \left(\frac{\Delta p}{\Delta p + k_p} \right)^{0.073} \tag{1}$$

where k_c=0.0250 m/s√Pa and k_p=1730 Pa for the EAS Fiberglass Company woven cloth used here.

Tests were performed using a 0.9-m chord DU91W250 airfoil model. This is a 25% thick wind turbine blade section with 1.6-mm thick trailing edge. The model was fabricated by stacking a series of 50-mm thick CNC-machined aluminum laminates. The laminates are held together in compression resulting in a smooth, continuous and hermetically sealed surface with streamwise steps between adjacent laminates of less than 0.05-mm in height. A sandwich of Teflon film and compressed acoustic foam covered by Mylar film was used to extend the ends of the 1.816-m span model by 12-mm to the floor and ceiling of the test sections and create an air-tight seal. The model is instrumented with 90 pressure taps centered on the model midspan and arranged in diagonal rows on both sides of the model at an angle of 15 degrees to the chordwise direction. The model was rotated to angle of attack about its quarter chord location. Measurements were performed both with the model clean and with it tripped, though only results for the clean airfoil are shown here. Natural transition on the clean airfoil was verified during testing using Naphthalene flow visualization.

Free-stream flow speed during the measurements in either test section was monitored using taps in the walls of the wind tunnel settling chamber and contraction, sensed using a Datametrics Barocel Pressure Sensor Type 590D with traceable calibration. Flow temperature was sensed with an Omega Thermistor type 44004 (accuracy ±0.2°C) and the ambient absolute pressure was determined using a Validyne DB-99 Digital Barometer (resolution 0.01" Hg). Pressure measurements on the airfoil, used to infer lift coefficient were made using an Esterline

9816/98RK pressure scanner system with a range of ±2.5psi and uncertainty of ±0.05% full scale. Drag measurements in the anechoic test section were made using a wake rake system placed 2.74m downstream of the model center of rotation. The rake consists of 113 Pitot probes and 7 Pitot static probes distributed across the full width of the test section on an aerodynamic support structure that can be traverse in the spanwise direction. Rake pressures are sensed using four DTC Initium ESP-32HD 32-channel pressure scanners with a range of ±2.5psi.

The 0.9m DU91W250 was tested in both the aerodynamic and anechoic test section at a nominal Reynolds number of $3x10^6$ and a nominal freestream velocity of 60m/s, in clean and tripped conditions between -13 and 11°. Drag data was obtained from spanwise scans covering 74% of the span starting 254mm and up to 1626mm from the floor of the test-section. Anechoic test section results were corrected for blockage and Kevlar window deflection and transpiration using the method of Devenport *et. al*. [1]. These data was validated by comparing to previous runs obtained in the aerodynamic test-section. Note that a -0.3° offset in the anechoic angle of attack was applied for the clean case only for consistency with previous data and numerical simulations. Otherwise, differences between the results for the two test sections were only noticeable beyond positive and negative stall.

3.0 COMPUTATIONAL METHODS AND APPROACH

Computational Fluid Dynamics (CFD) has been used to examine the origin of the anechoic test section aerodynamic corrections. Specifically the EllipSys code [4-6] developed at DTU over the past 25 years and applied for numerous wind energy related flows was used. Since wing sections are the main application in the Virginia Tech and the Poul la Cour Tunnel the corrections are demonstrated on such models. Predictions of the DU91W250 wing section in the Stability Tunnel were carried out at several angles of attack taking into account the existence of both solid walls and the flexible and porous Kevlar walls. The influence of the boundary conditions on the flow were investigated. The predicted flow in the test section is dependent on several parameters like the applied turbulence model, the inlet velocity profile, the numerical dissipation and the tested wing section type. These CFD predictions will be compared not only to measurements, but also to free-flight vortex panel method results. The CFD investigation was undertaken to reveal the influence of different types of boundary conditions and determine flow mechanisms that drive the aerodynamic corrections.

3.1 The EllipSys code

The EllipSys code is an incompressible multi-block Finite Volume code, based on the pressure correction approach, on curvilinear grids. EllipSys is used in Reynolds Averaged Navier-Stokes mode with the k-omega SST turbulence model [7]. The third order QUICK scheme by Leonard [8] is used for the convective terms, while the diffusive terms are modelled by second order accurate central differences.

3.2 Boundary conditions

Only the test section was modelled. The inlet to the domain was 3.325 m upstream of the airfoil leading edge and the outlet was 3.985 m downstream. The Kevlar wall condition was applied in the range of 1.775 m upstream to 2.585 m downstream. The height of the domain was 1.83 m. The domain consisted of 63,488 cells with a minimum cell height closest to the airfoil surface of 10^{-5}m resulting in $y^+<2$. Dirichlet conditions were applied at the inlet, while zero gradients were assumed at the outlet of the tunnel, for velocities and turbulence quantities. At the outlet the flux was scaled to equal the total flux through the inlet, while zero gradient of the pressure correction was assumed at all external boundaries. The pressure in contrast was found by second order extrapolation from the interior of the domain at all external boundaries.

Several types of approximations for the Kevlar walls were tested. Specifically we consider separately and together the effects of (a) applying a no-slip condition at the Kevlar walls (b) modelling their porosity, and (c) modelling their deformation under pressure loading. In the cases where the porosity effect was included, the transpiration velocity was found using Eqn.(1) from the difference between the computed wall pressure and an external reference pressure. The reference pressure, assumed the same for both Kevlar walls, was determined based on the requirement that any mass flow in through one of the walls be matched by mass flow out through

the other. Note that while this net zero mass flux condition was also required by the experimental setup, that setup also permitted differences in the exterior pressure on the two Kevlar windows (typically no more than a few percent of the dynamic pressure). This difference, accounted for in the inviscid panel method model used for aerodynamic corrections but not the CFD may have caused the CFD solution to slightly overestimate interference effects due to porosity.

The deformation of Kevlar walls, where needed, was modelled using 3D membrane theory, considering the modulus of the Kevlar, the pre-tensioning and the pressure difference between the test chamber and the anechoic chambers. An iterative method was used to couple the CFD and membrane calculations at a few angles-of-attack. Approximately five iterations were needed to obtain convergence in the pressure on the wall and the deformation. As the CFD simulations were two dimensional, in a plane perpendicular to the Kevlar walls, the average deflection across the width of the Kevlar window (2/3rds of the maximum deflection) was used to define the wall position in the CFD. The maximum deformation at 6 degrees angle of attack was found to be -6.1 cm of the wall with no slip porous condition on the suction side of the airfoil.

The far-field reference pressure (in contrast to the external reference pressure noted above) used when computing force coefficients and the pressure coefficients was determined at the inlet as the average pressure over the cross sectional area. In the experiment, the reference pressure was determined from ports placed in the wind tunnel settling chamber and contraction, and a calibration between these values and the pressure at the streamwise center of the empty test section where models are mounted. Thus the reference pressure and free stream velocity used in the experiments accounts for boundary layer growth on the test section walls from the inlet, whereas those used with the CFD do not.

4.0 RESULTS AND DISCUSSION

In this section results based on EllipSys are shown and compared to measurements from the Stability Tunnel. In section 4.1 free-flight simulations are compare to the measurements made in both hard and Kevlar-walled test sections. In 4.2 measurements in the Kevlar-walled test section are compared with simulations using different wall boundary conditions; slip/no slip, solid/Kevlar walls, deformed/non-deformed Kevlar walls. Here the flow in the test section including e.g. wall boundary layers, wall pressures is discussed. In all simulations, free transition at the airfoil was assumed. The transition process was modeled using the e^n-model of van Ingen [9], with the exponent n=9 (unless otherwise stated), which is a value commonly used for airfoil flow. All simulations were made with Reynolds number $3x10^6$ with a chord length of 0.9m and uniform velocity inlet velocity, consistent with the test conditions.

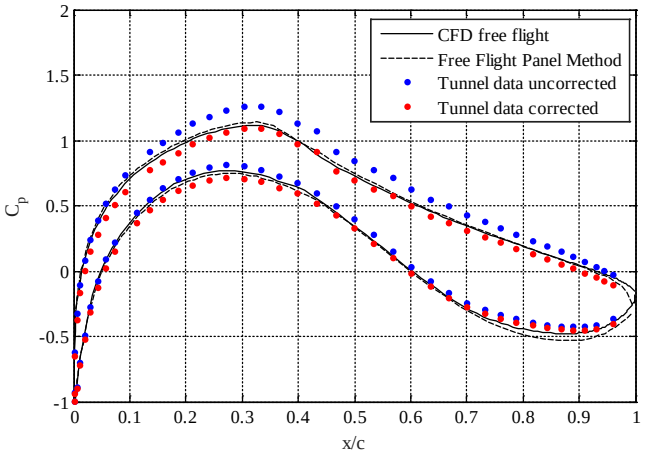

Figure 3 - Pressure coefficient distribution on the airfoil in free flight (CFD) compared with raw and corrected tunnel data taken in the Stability Tunnel hard-wall test section. Zero angle of attack.

4.1 Free flight calculations and corrected wind tunnel data

We assess the validity of the CFD simulation by comparing corrected wind tunnel measurements made on the DU91-W250 with free-flight calculations. Fig. 3 compares pressure distributions on the airfoil at zero angle of attack with measurements from the hard wall aerodynamic test section of the Stability Tunnel, corrected using standard methods [10]. Fig. 4 shows lift and drag coefficient as a function of angle of attack and includes measurements from the Kevlar-walled test section of the Stability Tunnel corrected using the method of Devenport *et al.* [1]. (Note that measurements for the hard wall configuration were not available for the drag comparison.) Good agreement between the CFD and corrected experimental data is seen at low angles-of-attack both in the pressure distributions and in the integrated coefficients. However at higher angles-of-attack, i.e. around maximum and minimum lift, some deviations are seen. In particular, the CFD seems to slightly over-predict lift the lift, while under-predicting the increase in drag with lift magnitude. Except in this regard, the plots show that the EllipSys code predicts the aerodynamic performance well and that the correction methods used for the solid wall and Kevlar wall configurations are appropriate and consistent. In the remainder of this paper we therefore focus on what the CFD reveals about the aerodynamics of the porous flexible Kevlar walls, and their impact on the flow around the model.

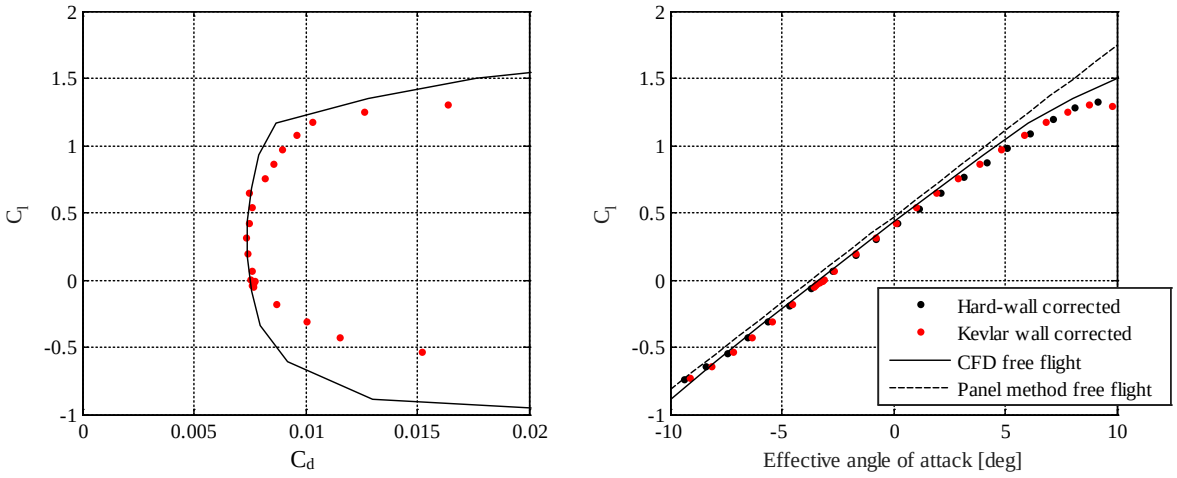

Figure 4 – Lift and drag coefficients compared with CFD free flight calculation. Natural transition (*n*=9)

4.2 Investigation of boundary conditions for the Kevlar test section

In this section we compare uncorrected measurements made in the Kevlar walled test section with EllipSys calculations made incorporating different components of the anechoic test section boundary conditions. Computational cases considered include:

1) No slip solid walls. Test section is modeled as if it were hard wall.
2) Slip solid walls. Test section modeled as hard wall, but no-slip condition on the walls is ignored.
3) No slip porous walls. Kevlar porosity is modelled but deflection is not.
4) Slip porous walls. Kevlar porosity is modelled but deflection is not, and the no-slip condition is ignored.
5) No slip porous deformed walls. Kevlar porosity and deformation are modelled.

Calculations were performed over a range of angles of attack depending on condition. The detailed comparisons shown below will mostly focus on angles of attack of -3.2, 0 and 6 degrees.

Fig. 5 compares integrated lift and drag measurements with calculations for all conditions listed above. Looking at the lift results (Fig. 5(b)) the accuracy of the computed results for the most part increases as more aspects of the true boundary condition are included. The no-slip porous wall case (which includes all but the deformation) predicts a lift curve that falls only slightly below that of the measurements at most angles of attack.

This is consistent with the fact that the neglected deformation effects would tend to slightly increase the measured lift. However, the CFD for the no-slip porous deformed wls case, representing the complete modeling of the boundary condition, seems to over-correct for this effect, particularly at 6 degrees.

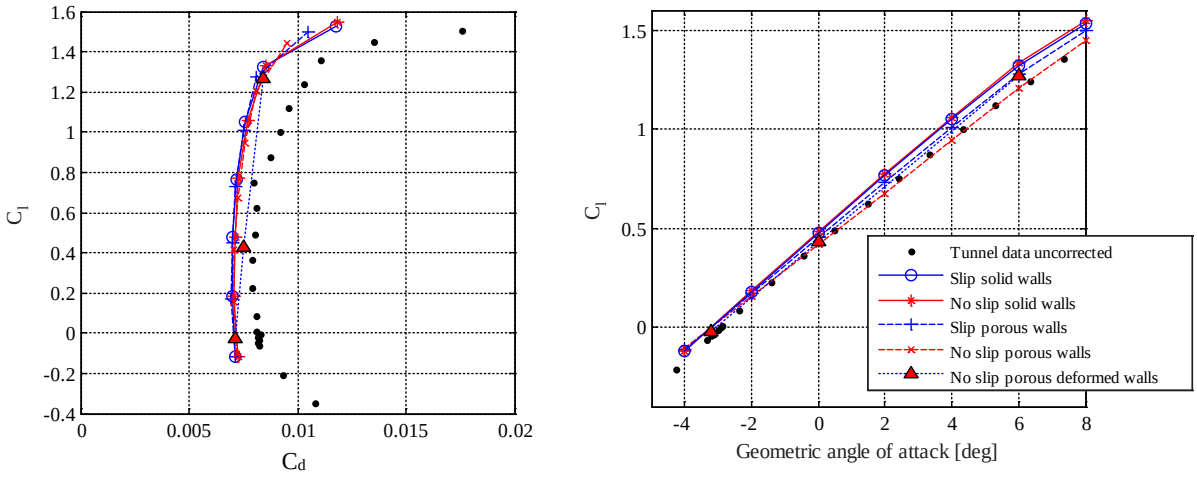

Figure 5 – Force coefficients on the airfoil for case of natural transition (n=9) with varying tunnel wall boundary conditions. Re = 3x10^6

Fig. 5(a) shows that the various boundary conditions have relatively little effect on the predicted drag.

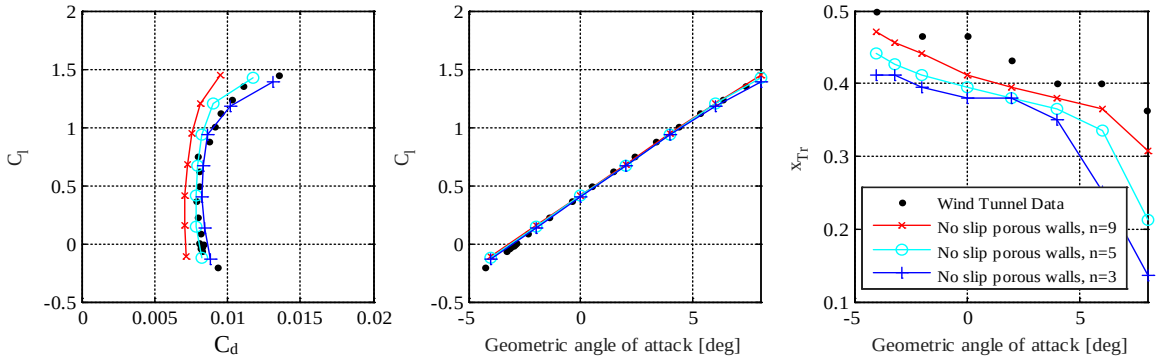

Figure 6 – Comparison of values of the transition exponent *n*, for the no-slip porous wall case.

Predicted drag levels are all substantially below those measured. Note that the drag forces from the computations were obtained using a numerical wake-rake approach and by using Jones' equation [11] to resemble the method used in the experiments. One possible explanation for this discrepancy is inaccuracy in the transition predictions. In **Figure** the measurements are compared to simulations for the no-slip porous wall case, with different exponent values in the e^n model. Results using three n values are shown: n=9, 5 and 3, which nominally correspond to free stream turbulence intensities of 0.070%, 0.371% and 0.854%, respectively. These turbulence intensities are all higher than expected levels in the Virginia Tech Stability Tunnel. The difference in the lift coefficient is very small whereas the difference in drag coefficient is significant. This plot appears to show that the drag discrepancy may be due to more rapid transition on the model than in the CFD. However, this hypothesis is not supported by a comparison between transition locations shown in Fig. 6(c). Measured transition locations are clearly *downstream* of those predicted, implying a value of n of about 10. This discrepancy remains unresolved. Nevertheless, this discussion highlights the importance of free stream turbulence levels in correlating measurement and CFD, and thus effects of the model and test conditions on those turbulence levels, which are often not documented experimentally.

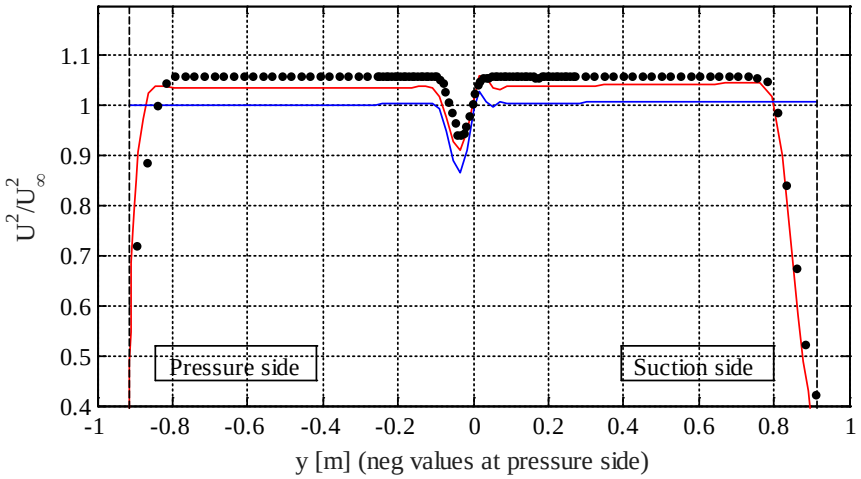

Figure 5 - Comparison of profiles of dynamic pressure ratio downstream of the airfoil computed with the slip and no-slip porous wall boundary condition as well as experimental data at 0 degrees. Data are obtained at 2.74m downstream of the model center of rotation.

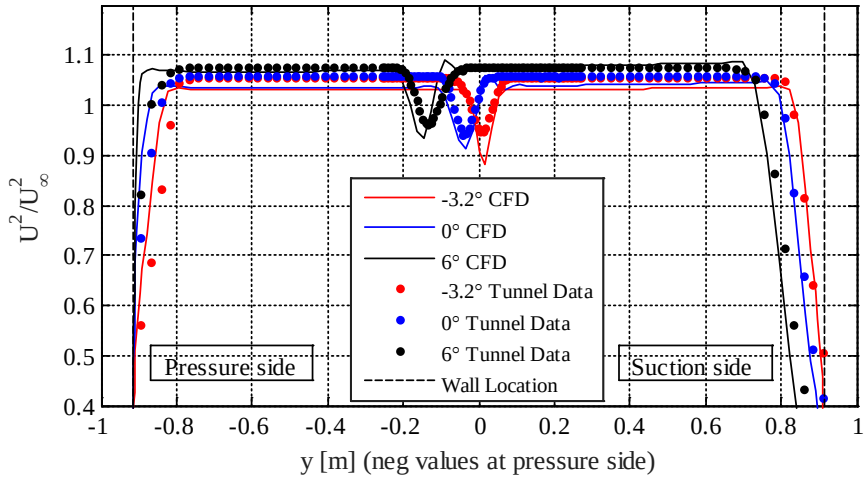

Figure 6 - Comparison of profiles of dynamic pressure ratio downstream of the airfoil between the no-slip porous wall simulation and experimental data at angles of attack of -3.2 (zero-lift), 0, and 6 degrees

Figs. 7 and 8 show the calculated effects of the no slip and porosity boundary conditions on dynamic pressure profiles downstream of the airfoil at the wake rake location, ignoring deformation. Fig. 7 shows results for zero angle of attack. Both the slip porous wall and no-slip porous wall cases appear to show fairly accurate predictions of the wake profile. However, without a no-slip condition, no wall boundary layers are predicted, and thus the blockage effect of these boundary layers in speeding up the potential core is missed. It is therefore clear that the no slip condition is needed, implicitly or explicitly, in describing the boundary conditions. However, even though the overall agreement of the profile is better in the no slip case there are small differences such as the dynamic pressure that is predicted around 2% smaller outside the boundary layers and the wake. This appears to be connected to an under prediction of the test section wall boundary layer thickness on the pressure (negative y) side. Note that in the panel method of [1] and [3] the no-slip condition is crudely modelled by doubling the transpiration mass flow rate into the test section. The rationale here is that flow that enters via transpiration has zero streamwise momentum, and a displacement volume roughly twice that implied by its mass flow rate.

Figure 6 compares measurements for -3.2°, 0° and 6° angle of attack with the no-slip porous wall calculation. It is seen that if the angle-of-attack is changed the agreement is still good when assuming no slip condition at the

walls. However discrepancies are visible. For example, the boundary layers at the wall appear to deviate from the experimental results as the angle-of-attack is increased, possibly caused by over-prediction of the transpiration at higher angles-of-attack. Thus, for increasing angle of attack the predicted boundary layer at the wall on the suction side becomes thicker compared to measurements and at the pressure side it becomes thinner. This over-prediction of the transpiration could be due to the fact that the reference pressures in the two anechoic chambers are assumed the same in the computations, but are slightly different in the measurements, with a pressure that is lower outside the suction-side wall and higher outside the pressure-side wall.

Figs. 9 and 10 show the effects of porosity and wall deformation in terms of pressure distributions along the insides of the pressure and suction-side Kevlar walls. No wall pressure measurements were made but these plots include pressures calculated using the inviscid panel method approach of [1] and [3] with both porosity and wall deformation effects included. Negative pressure coefficient is plotted as a function of axial position relative to the airfoil leading edge location for 0 and 6 degrees angle of attack. The effects of porosity on the wall pressures appear relatively minor on the pressure side wall, as results for no-slip solid walls and no slip porous walls appear quite similar. On the suction side, however, porosity noticeably reduces the pressure coefficient (making $-C_p$ bigger) downstream of the airfoil. Presumably this is blockage associated with transpiration into the test section under the low wall pressures produced in the vicinity of the airfoil. Adding deformation increases the magnitude of the wall pressure variations on the suction side of the test section and amplifies this downstream blockage effect (Figs. 9(b) and 10(b)). The inviscid panel method calculation appears to match the CFD results for deformation and porosity quite well upstream of the airfoil, but does not reproduce the blockage effect downstream. This could be taken to indicate the importance of the no-slip condition in modeling this effect, but may also reflect differences in how the mass flow balance through the Kevlar walls was handled. It remains an open issue whether or not it is necessary to adapt the CFD turbulence model to account for the porous wall.

In **Figure 11** the pressure distributions predicted by CFD are compared with measurements made in the anechoic test section for angles-of-attack of 0° and 6°. At both angles-of-attack the most accurate predictions correspond to the no-slip porous wall case, where the porosity is modelled but not the deformation. In this case the predicted $-C_p$ lies slightly above that measured on both sides of the airfoil, as though the solid blockage produced by the airfoil is being slightly over-predicted in the CFD. Adding deformation to the calculation (no-slip porous deformed walls) only magnifies this discrepancy since, as noted earlier the deformation of the walls is counter to the overall curvature of the streamlines produced by the airfoil. One could argue that, at least at 6°, this effect is consistent with the slight over prediction of the suction side boundary layer thickness seen in Fig. 8, since this implies greater viscous blockage in the no-slip Kevlar calculation than in the measurement.

5.0 CONCLUSIONS AND FURTHER WORK

Boundary conditions used in prediction of a DU91-W250 have been investigated for a porous flexible Kevlar wall acoustic test section. Measurements were made in the Virginia Tech Stability Wind Tunnel and compared to two-dimensional CFD predictions made using the EllipSys2D code developed by DTU. Overall, the agreement between measurements and computations was good, the CFD quite accurately reproducing the lift behavior of the airfoil, its pressure distributions, velocity profiles measured through the airfoil wake, and wind tunnel wall boundary layers downstream. In addition to the porosity and deformation of the Kevlar walls, it was found that the no slip condition at the test section walls was needed to get a fair agreement with the measurements. However, the exact pressure difference over the Kevlar wall also plays a significant role in determining the aerodynamic corrections. This could be one of the reasons that the CFD assuming no slip conditions and deformable porous walls over-predicted the pressures at higher angles of attack. Also, the pressure difference over the wall is an important aspect of the flow through the test section which is only crudely modeled in the current standard panel method correction scheme.

The comparisons also highlighted some specific issues that need to be investigated further in the near future. The CFD consistently under-predicted drag while predicting transition locations upstream of those measured for reasons that are not clear at present. Calculations also showed slightly larger blockage effects on the airfoil

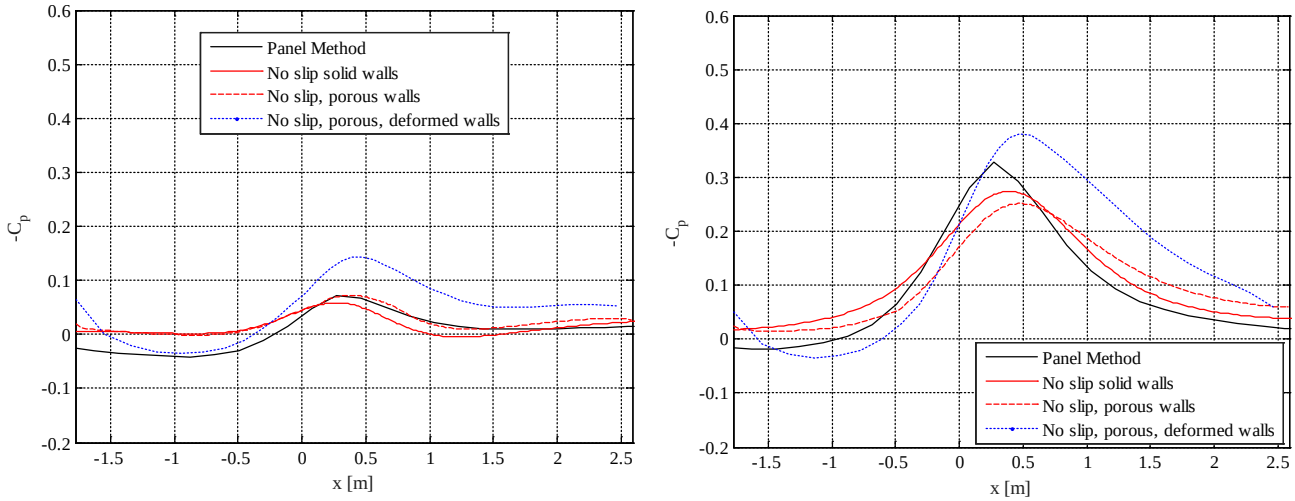

Figure 9 - Pressure distributions along the test section wall at zero angle of attack predicted by panel code and CFD, respectively. Left - pressure side and right - suction side.

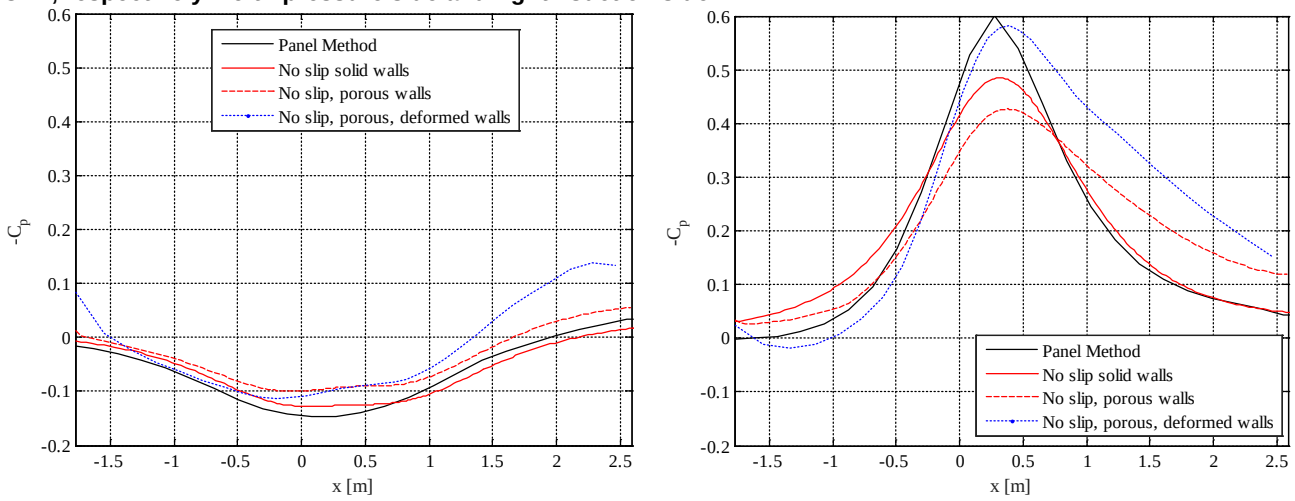

Figure 10 - Pressure distributions along the test section wall at 6 degrees angle of attack predicted by panel code and CFD, respectively. Left - pressure side and right - suction side.

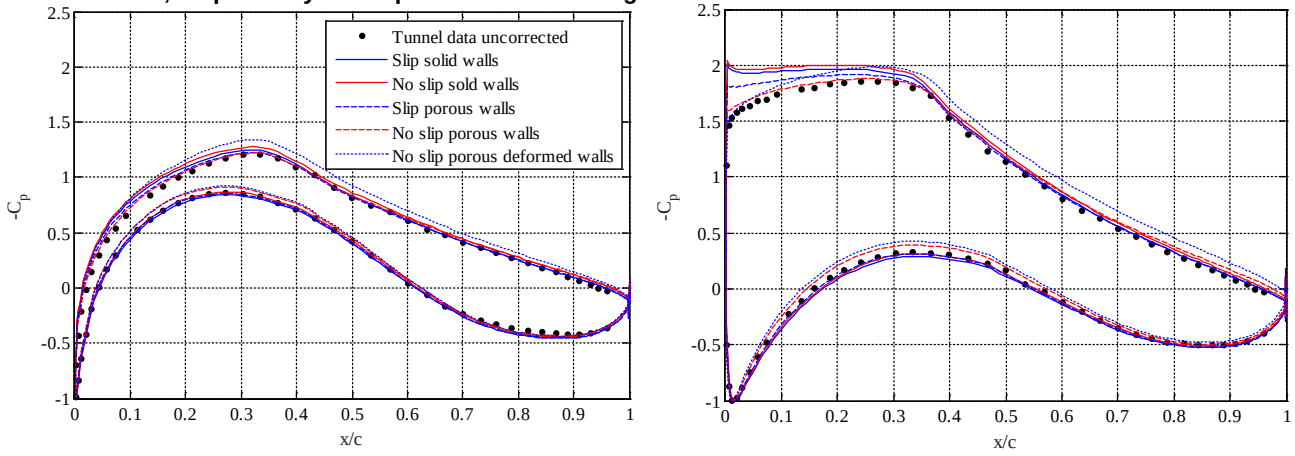

Figure 11 Pressure distribution on airfoil under deformed and non-deformed CFD configurations of Kevlar walls compared with tunnel data. Left 0 deg. and right AOA=6 deg. angle of attack.

pressure distributions than those measured. This may be the result of an over-estimate of the blockage associated with transpiration velocity through the wall.

In the longer term we see this work extending in several directions. First calculations need to be extended to three dimensions. The comparisons presented here and elsewhere suggest that the boundary layers formed over the acoustically treated floor and ceiling of the test section, and the junction flows formed where those surfaces meet with a model, do not exert a dominant effect on aerodynamic measurements. However, this needs to be directly demonstrated and any secondary effects assessed against the effects of the Kevlar walls themselves. Second, additional measurements need to be made to compare with predictions. The measurement of pressure distributions over the Kevlar walls and the resulting deflections they produce can be made [3] and would directly benefit the comparisons with CFD. The measurement of free stream turbulence levels, during the model test, would also reduce uncertainty in CFD transition modeling. Third, acoustic calculations of the airfoil trailing edge noise, coupled with measurements and estimates of the facility Green's function would provide the means to validate sound as well as flow performance. Finally, progress is needed to incorporate CFD approaches as part of *a priori* free flight corrections. Such a procedure would use CFD for high fidelity modeling of the test section and walls, while requiring that the influence of a model be incorporated through measured bulk aerodynamic characteristics.

ACKNOWLEDGEMENTS

We would like to thank Erwan Jézéquel (Ecole Centrale de Lille) for setting up the 2D CFD computations and carry out the initial computations in an internship at DTU Wind Energy. We would also like to thank Nanya Intaratep, Tim Meyers and Bill Oetjens for their assistance in the Stability Tunnel experiments.

REFERENCES

1. Devenport, W.J., Burdisso, R.A., Borgoltz, A., Ravetta, P.A., Barone, M.F., Brown, K.A., and Morton, M.A., *The Kevlar-walled anechoic wind tunnel.* Journal of Sound and Vibration, 2013. **332**(17): p. 3971-3991.
2. Ito, T., Ura, K., Nakakita, K., Yokokawa, Y., Ng, W.F., Burdisso, R., Iwasaki, A., Fujita, T., Ando, N., Shimada, N., and Yamamoto, K., *Aerodynamic/Aeroacoustic testing in Anechoic Closed Test Sections of Low-speed Wind Tunnels*, in *16th AIAA/CEAS Aeroacoustics Conference*. 2010: Stockholm, Sweden.
3. Brown, K.A., *Understanding and Exploiting Wind Tunnels with Porous Flexible Walls for Aerodynamic Measurement*, PhD, *Aerospace and Ocean Engineering*. 2016, Virginia Tech.
4. Sørensen, N.N., *General purpose flow solver applied to flow over hills*. 1995, Risø National Laboratory.
5. Michelsen, J.A., *Basis3D - A Platform for Development of Multiblock PDE Solvers*. 1992, Technical University of Denmark.
6. Michelsen, J.A., *Block Structured Multigrid Solution of 2D and 3D Elliptic PDE's*. 1994, Technical University of Denmark.
7. Menter, F.R., *Zonal Two Equation k-ω Turbulence Models for Aerodynamic Flows*, in *24th AIAA Fluid Dynamics Conference*. 1993: Orlando, FL.
8. Leonard, B.P., *A stable and accurate convective modelling procedure based on quadratic upstream interpolation.* Computer Methods in Applied Mechanics and Engineering, 1979. **19**(1): p. 59-98.
9. van Ingen, J.L., *Theoretical and Experimental Investigations of Incompressible Laminar Boundary Layers with and Without Suction*. 1965, Technical University of Denmark
10. Allen, H.J. and Vincente, W.G., *Wall Interference in a Two-Dimensional-Flow Wind Tunnel, With Consideration of the Effect of Compressibility*. 1947, NACA.
11. Jones, M., *The measurement of profile drag by the Pitot-traverse method, Reports and Memoranda*. 1936, Cambridge University Aeronautics Laboratory.